Increased Fanconi C expression contributes to the emergency granulopoiesis response

Liping Hu,[1] Weiqi Huang,[1,2] Elizabeth Hjort,[1] and Elizabeth A. Eklund[1,2]

[1]Feinberg School of Medicine and Robert H. Lurie Comprehensive Cancer Center, Northwestern University, Chicago, Illinois, USA.
[2]Jesse Brown VA Medical Center, Chicago, Illinois, USA.

Emergency granulopoiesis is a component of the innate immune response that is induced in response to infectious or inflammatory challenge. It is characterized by the rapid expansion and differentiation of granulocyte/monocyte progenitor (GMP) populations, which is due in part to a shortened S-phase of the cell cycle. We found that IRF8 (also known as ICSBP), an interferon regulatory transcription factor that activates phagocyte effector genes during the innate immune response, activates the gene encoding Fanconi C (*Fancc*) in murine myeloid progenitor cells. Moreover, IRF8-induced *Fancc* transcription was augmented by treatment with IL-1β, an essential cytokine for emergency granulopoiesis. The Fanconi pathway participates in repair of stalled or collapsed replication forks during DNA replication, leading us to hypothesize that the Fanconi pathway contributes to genomic stability during emergency granulopoiesis. In support of this hypothesis, *Fancc*$^{-/-}$ mice developed anemia and neutropenia during repeated, failed episodes of emergency granulopoiesis. Failed emergency granulopoiesis in *Fancc*$^{-/-}$ mice was associated with excess apoptosis of HSCs and progenitor cells in the bone marrow and impaired HSC function. These studies have implications for understanding the pathogenesis of bone marrow failure in Fanconi anemia and suggest possible therapeutic approaches.

Introduction

The interferon consensus sequence binding protein (ICSBP) is an interferon regulatory transcription factor that was cloned by homology to interferon regulatory factors 1 and 2 (referred to as ICSBP or IRF8) (1). IRF8 is expressed in HSCs, myeloid and B progenitor cells, and mature phagocytes and B cells. IRF8 activates transcription of a number of genes that encode phagocyte effector proteins, including *gp91*^{phox}, *p67*^{phox}, and IL-18 (2–4). In previous studies, we found that IRF8 contributes to phagocyte function during the innate immune response by activating these genes (2, 3). A murine model with *Irf8* gene disruption provided additional clues regarding IRF8 function (5, 6). In these studies, the biology of IRF8-deficient mice was dominated by mild steady-state granulocytosis (5, 6). However, these mice were susceptible to infection due to impaired B cell and phagocyte function (5, 6). And *Irf8*$^{-/-}$ mice failed to develop leukocytosis during infectious challenge and succumbed rapidly to overwhelming infection (i.e., impaired emergency granulopoiesis).

Emergency granulopoiesis (or stress granulopoiesis) is a specific response to infectious or inflammatory challenge and represents an essential component of the innate immune response. In contrast, steady-state granulopoiesis is an ongoing process that replaces neutrophils depleted by the normal programmed cell death. During the first hours after infectious challenge, emergency granulopoiesis is characterized by an increase in circulating neutrophils due to vascular demargination and release from the bone marrow. This process is maximal in 24 hours after infection. Subsequently, accelerated differentiation and expansion of HSC and granulocyte/monocyte progenitor (GMP) populations in the bone marrow occurs. Expansion of these progenitor populations is due, in part, to shortened S-phase of the cell cycle. This proliferative phase of emergency granulopoiesis is maximal at 10 to 14 days (7, 8).

Emergency granulopoiesis and steady-state granulopoiesis are controlled by different molecular mechanisms. Murine genetic studies determined that STAT3 and C/EBPβ are required for emergency granulopoiesis but are dispensable for steady-state granulopoiesis (9, 10). Murine studies also demonstrated that the IL-1 receptor (IL-1R) is essential for emergency, but not steady-state, granulopoiesis (7). Disrupting the gene encoding G-CSF decreased emergency granulopoiesis but did not abolish the response (11, 12). This is of interest, because IL-1β is required for the increase in G-CSF expression that is observed during emergency granulopoiesis (8, 13).

In previous chromatin immunoprecipitation–based screening studies, we identified a set of IRF8 target genes that are involved in regulating granulopoiesis and the innate immune response. This set included genes that terminate cytokine-induced proliferation (*NF1* and *GAS2*), increase sensitivity of phagocytes to Fas-induced apoptosis (*PTPN13*), and are involved in DNA repair (*FANCF*) (14–17). We found that IRF8 activated *FANCF* (the gene encoding Fanconi F) in bone marrow progenitor cells that were stimulated with differentiating cytokines (17). In this study, we determined that IRF8 also controls the gene encoding Fanconi C (*FANCC*). Based on these results, we considered the possibility that IRF8 protects cells from the genotoxic stress of myelopoiesis by controlling a DNA repair pathway. Because of the functional connection between IRF8 and the innate immune response, we hypothesized that IRF8-induced Fanconi expression might be especially relevant to emergency granulopoiesis.

The Fanconi DNA repair pathway includes 15 proteins (also referred to as complementation groups), and absence of any of complementation group results in Fanconi anemia (FA) (18, 19). Fanconi proteins are characterized as core (Fanconi A, B, C, E, F, G, M, N), substrate (Fanconi D2 and I), or effector (Fanconi D1, J, L, O, P) proteins. Assembly of the core complex results in monoubiquitination of Fanconi D2 and I, which results in assembly on DNA of a homologous recombination repair (HRR) complex that includes Fanconi O, P, and J as well as RAD51 and the MRE11-

Conflict of interest: The authors have declared that no conflict of interest exists.
Citation for this article: *J Clin Invest.* 2013;123(9):3952–3966. doi:10.1172/JCI69032.

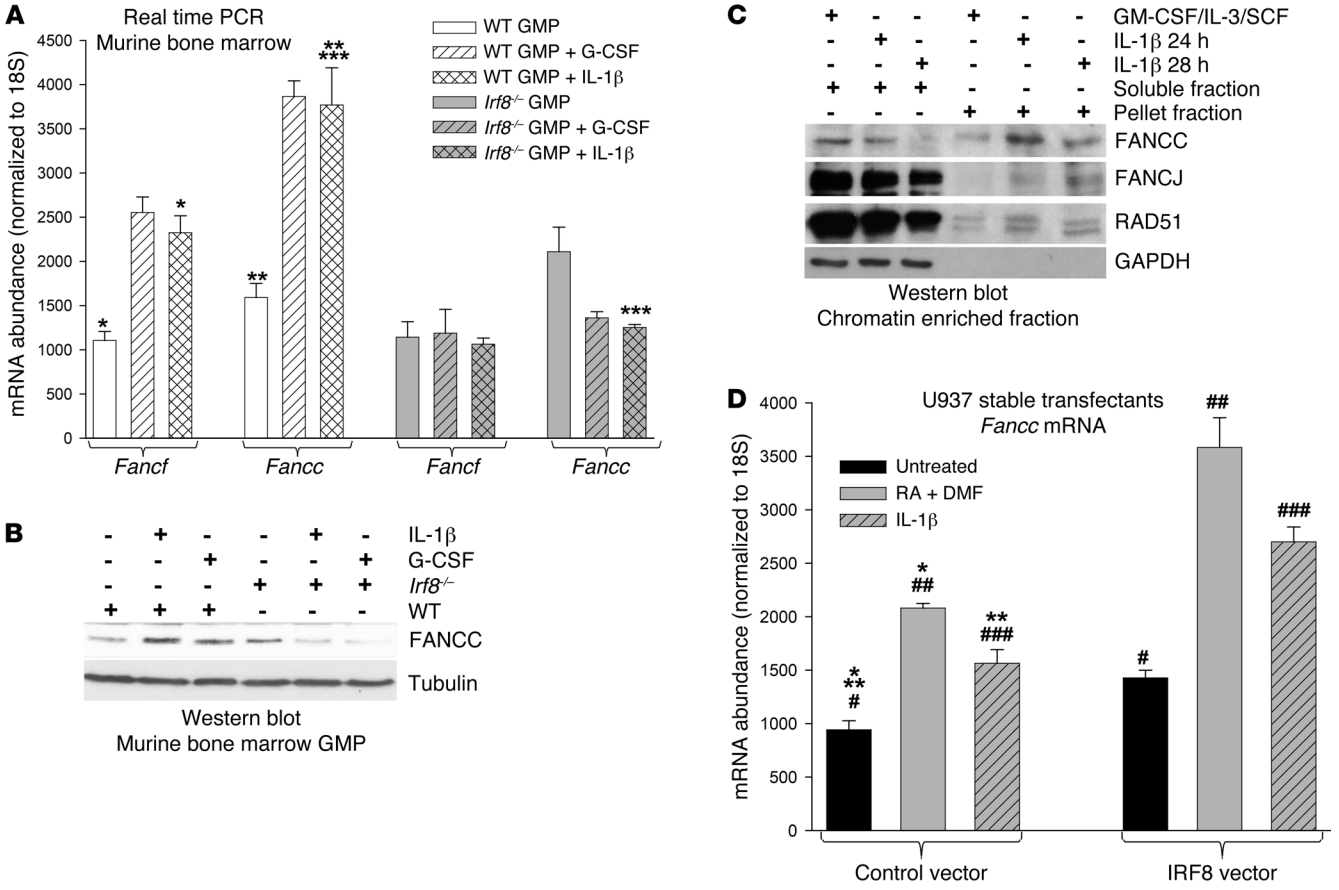

Figure 1

IRF8 influences FANCC expression in myeloid progenitor cells. (**A**) IL-1β or G-CSF increase *Fancc* mRNA expression in myeloid progenitor cells from WT mice but not *Irf8*$^{-/-}$ mice. Bone marrow from WT or *Irf8*$^{-/-}$ mice was cultured under GMP conditions (enriched for CD34^{+} cells). Some cells were treated with IL-1β or G-CSF. *Fancc* and *Fancf* mRNA was quantified by real-time PCR. Statistically significant differences in expression with versus without differentiation are indicated by $^{*}P < 0.01$ or $^{**}P < 0.01$ and with versus without IRF8-knockout by $^{***}P < 0.01$. There was no significant difference between IL-1β versus G-CSF induced expression ($P > 0.1$). (**B**) IL-1β increases FANCC protein in WT but not *Irf8*$^{-/-}$ myeloid progenitor cells. The cells were analyzed by Western blots serially probed with antibody to FANCC and tubulin (loading control). (**C**) IL-1β increases FANCC, FANCJ, and RAD51 in the chromatin-enriched cell fraction. Bone marrow CD34^{+} cells from WT mice were treated with IL-1β for 24 or 48 hours, and chromatin and soluble fractions were evaluated by Western blots serially probed with antibodies to FANCC, FANCJ, RAD51, and GAPDH (loading control). (**D**) IL-1β and retinoic acid increase *Fancc* mRNA expression in U937 myeloid leukemia cells. U937 cells were stably transfected with an IRF8 expression vector or control vector. Cells were treated with IL-1β or RA/DMF, and *Fancc* mRNA was quantified by real-time PCR. Statistically significant differences in expression with versus without differentiation are indicated by $^{*}P < 0.01$ or $^{**}P < 0.01$ and with versus without IRF8 overexpression by $^{\#}P < 0.01$, $^{\#\#}P < 0.01$, or $^{\#\#\#}P < 0.01$.

RAD50-NBS11 (MRN) complex (reviewed in refs. 18–20). The Fanconi pathway also participates in DNA repair through translesional synthesis (TLS) (20). In this case, the Fanconi core proteins interact with Polζ and Rev1 to activate BRCA1 and FANCJ (20). Since the Fanconi pathway is nonredundant for HRR and TLS, deficiency of any Fanconi protein causes defective DNA cross-link repair (21). Recent studies identified repair of stalled or collapsed replication forks as major functions of the Fanconi pathway (22, 23). Consistent with this, Fanconi D2 (FANCD2) associates with DNA during S-phase, even without DNA damage (24).

FA is a genetic disorder with variable phenotype that is characterized by bone marrow failure in childhood (18, 19). This may be due to apoptosis of HSCs and/or committed progenitor cells with damaged DNA. Patients who survive the bone marrow failure phase of FA frequently develop myelodysplasia and progress to acute myeloid leukemia (AML). This is hypothesized to occur as mutations accumulate in genes that regulate cell cycle checkpoints and the apoptotic responses to DNA damage (25, 26). The hypothesis of these studies is that IRF8-induced expression of Fanconi proteins facilitates repair of stalled or collapsed replication forks during shortened S-phase of emergency granulopoiesis. If this hypothesis is correct, absence of Fanconi proteins would result in a failed emergency granulopoiesis response. We investigate this hypothesis using a Fanconi C–deficient (FANCC-deficient) murine model.

Results

IRF8 influences expression of FANCC. We previously determined that treatment of myeloid progenitor cells with differentiating cytokines increased expression of FANCF (17). In this study, we considered the possibility that these cytokines also induce expression of other Fanconi proteins. To investigate this, CD34^{+} cells

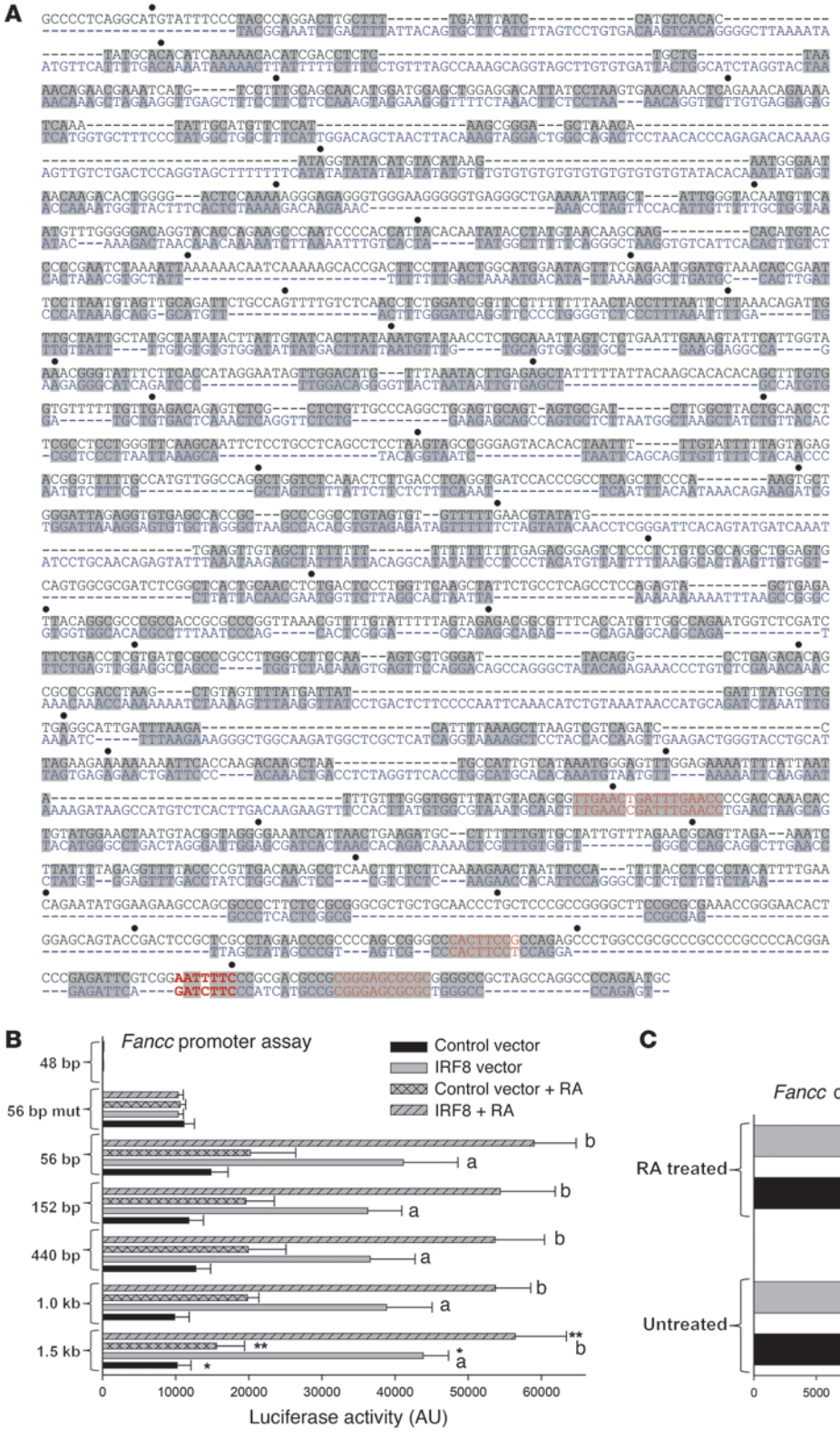

Figure 2

IRF8 activates a cis element in the proximal *Fancc* promoter. (**A**) The *Fancc* 5′ flank has conserved consensus sequences for interferon regulatory factor binding. The human (black) and murine (blue) *Fancc* 5′ flanks were compared for conserved consensus sequences for interferon regulatory factor binding. The identified sequences are indicated in red. Every 50 bp, counting from the transcription start site, are indicated by a black circle. (**B**) IRF8 activates the *Fancc* promoter. U937 myeloid cells were cotransfected with reporter constructs containing truncations of the *Fancc* 5′ flank and a vector to express IRF8 (or control vector). Reporter gene activity was determined with or without RA/DMF treatment. Reporter gene activity that is not significantly different within groups is indicated by a or b. Statistically significant differences with versus without IRF8 overexpression are indicated by $^{*}P < 0.01$ and $^{**}P < 0.01$. (**C**) IRF8 activates a cis element found between –56 and –48 bp of the *Fancc* promoter. U937 cells were cotransfected with a reporter construct with 3 copies of the –58- to –46-bp sequence of the *Fancc* promoter linked to a minimal promoter and a vector to express IRF8 (or relevant control vectors). Reporter gene activity was determined with or without RA/DMF. Statistically significant differences with versus without IRF8 overexpression are indicated by $^{*}P < 0.01$ or $^{***}P < 0.01$ and with versus without differentiation by $^{**}P < 0.01$.

were isolated from the bone marrow of C57 Black 6 mice and cultured in GM-CSF, IL-3, and SCF. This population was enriched for GMP cells ($SCA1^{-}KIT^{+}CD34^{+}CD38^{-}GR1^{-}$) (16, 27). Some cells were cultured under these conditions (referred to as GMP culture conditions), followed by treatment with emergency granulopoiesis–related cytokines, IL-1β or G-CSF. Cytokine treatment induced differentiation of cultured cells (increase in $CD34^{-}CD38^{+}GR1^{+}$ cells), as previously demonstrated (28, 29).

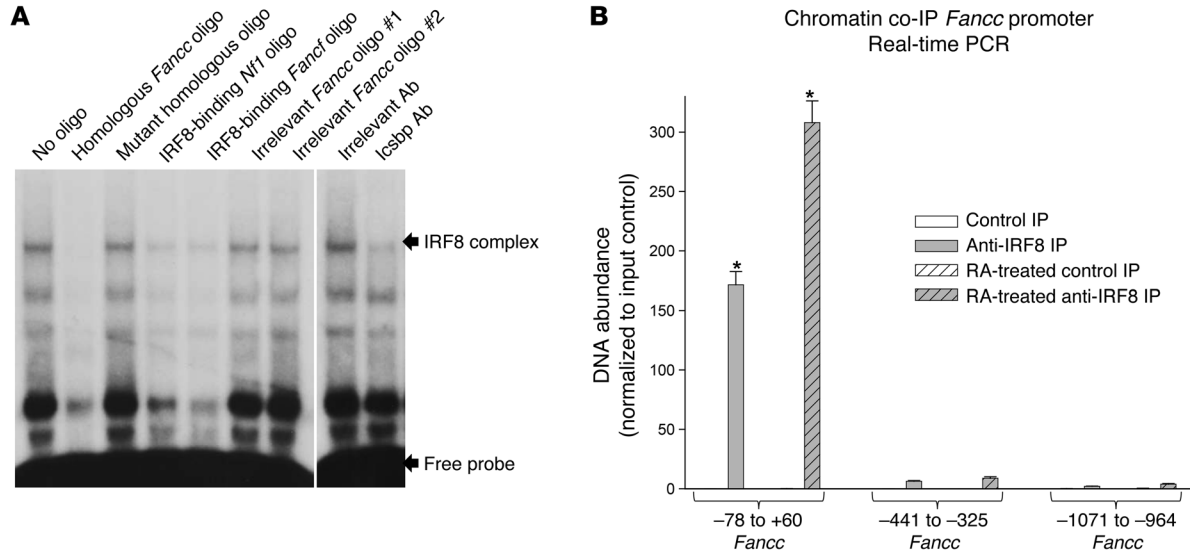

Figure 3

IRF8 binds to the proximal *Fancc* promoter cis element. (**A**) IRF8 binds to the –58- to –46-bp sequence of the *Fancc* promoter in vitro. EMSAs were performed with nuclear proteins from U937 cells and synthetic oligonucleotide probe representing the –56- to –46-bp sequence of the *Fancc* promoter. Binding assays were incubated with antibodies or double-stranded oligonucleotide competitors, as indicated. The IRF8 complex and free probe are indicated by arrows. (**B**) IRF8 binds to the *Fancc* promoter cis element in vivo. Chromatin coimmunoprecipitation was performed with U937 cells and an antibody to IRF8 (or control antibody). Cells were analyzed with or without RA/DMF treatment. Immunoprecipitated chromatin was amplified by quantitative real-time PCR with primers that flanked various sequences in the *Fancc* 5′ flank. Statically significant difference with versus without differentiation is indicated by **P* < 0.01.

Cells were analyzed by real-time PCR for expression of 2 Fanconi core proteins (FANCF and FANCC) and a Fanconi substrate protein (FANCD2). We found that treatment with IL-1β or G-CSF significantly increased *Fancf* or *Fancc* mRNA ($P < 0.001$, $n = 6$) (Figure 1A). There was no statistically significant difference in expression of *Fancf* or *Fancc* mRNA in cells treated with these 2 cytokines ($P > 0.1$, $n = 6$). In contrast, expression of FANCD2 was not consistently altered by either cytokine (data not shown). We also studied bone marrow from *Irf8*$^{-/-}$ mice to investigate the role of IRF8 in FANCC expression. For these experiments, we used *Irf8*$^{-/-}$ mice in proliferative phase (i.e., granulocytosis with mature neutrophils; prior to development of blast crisis) (6, 30). We found no statistically significant difference in *Fancf* and *Fancc* mRNA in WT bone marrow cells cultured under GMP conditions in comparison with similarly cultured *Irf8*$^{-/-}$ cells (Figure 1A). However, unlike WT cells, treatment of *Irf8*$^{-/-}$ cells with G-CSF or IL-1β did not increase expression of *Fancf* or *Fancc* mRNA. Differences in FANCC expression in *Irf8*$^{-/-}$ versus WT cells were also present at the protein level (Figure 1B).

In control experiments, we found that *Irf8*$^{-/-}$ murine bone marrow cells exhibited the same immunophenotype as WT cells under GMP culture conditions (as in our previous studies and those of others; refs. 6, 28–30). This was consistent with intact steady-state granulopoiesis in *Irf8*$^{-/-}$ mice prior to accumulation of mutations leading to blast crisis, as previously demonstrated (6, 30). Also similar to WT cells, treatment of *Irf8*$^{-/-}$ murine myeloid progenitor cells with IL-1β or G-CSF increased expression of cell surface markers associated with granulocyte maturation (>80% CD34^{-}CD38^{+}GR1^{+} cells at 48 hours, as for WT cells). This was consistent with a more specific role for IRF8 in FANCC or FANCF expression, rather than a more general effect of IRF8 on differentiation block.

Since expression of 2 Fanconi core proteins was increased by treatment of bone marrow progenitor cells with IL-1β or G-CSF, we hypothesize that the Fanconi pathway might be activated during emergency granulopoiesis. To investigate this, WT murine bone marrow cells were cultured under GMP conditions, followed by treatment with IL-1β for 24 or 48 hours. Cells were fractionated into chromatin-enriched versus soluble components, and proteins were analyzed by Western blot (31). We found that 24 hours of IL-1β treatment increased FANCC protein in the chromatin-enriched fraction of these cells, accompanied by a decrease in FANCC in the soluble fraction (Figure 1C). We also found that IL-1β treatment increased RAD51 and FANCJ proteins in the chromatin-enriched fraction and decreased these proteins in the soluble fraction (Figure 1C). This experiment was repeated twice, and a representative blot is shown (Figure 1C). RAD51 is associated with HRR, and FANCJ is associated with HRR and TLS (18–20), suggesting both DNA repair mechanisms may be activated during emergency granulopoiesis.

To identify a cell line model for *Fancc* promoter analysis, we also investigated *Fancc* mRNA expression in U937 leukemia cells. These cells are myelomonocytic progenitors that undergo granulocyte differentiation in response to various agents, including retinoic acid and dimethyl formamide (RA/DMF) or IL-1β (32). We generated IRF8-overexpressing stable U937 transfectants and analyzed Fanconi expression with or without IL-1β or RA/DMF. We found significantly more *Fancc* expression in IRF8-overexpressing transfectants in comparison with that in transfectants with control vector (~50% increase with IRF8 overexpression versus control, $P < 0.001$, $n = 4$) (Figure 1D). Treatment with IL-1β or RA/DMF further increased *Fancc* mRNA in IRF8-overexpressing transfectants ($P < 0.001$, $n = 4$) (Figure 1D) and augmented the difference

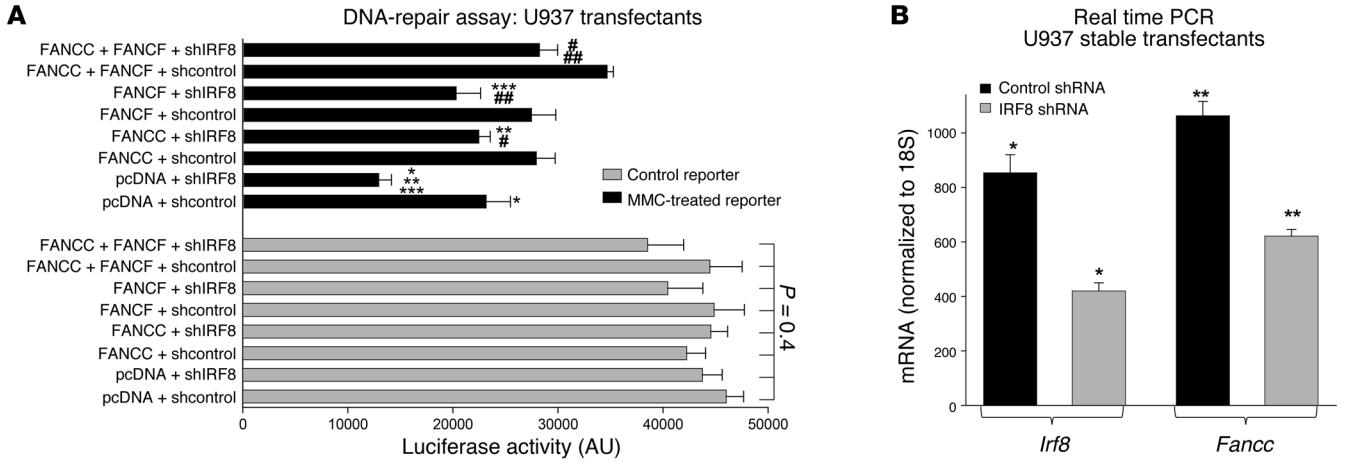

Figure 4

FANCC reexpression rescues DNA repair in IRF8-deficient cells. (**A**) IRF8 knockdown decreases repair of MMC-damaged plasmid in U937 transfectants, and this is reversed by FANCC and/or FANCF expression. U937 cells were stably transfected with a vector to express an IRF8-specific shRNA or scrambled control shRNA. These cells were cotransfected with a reporter plasmid and a vector to express FANCC, FANCF, FANCC plus FANCF, or empty vector control. Some reporter plasmids were pretreated with MMC to generate DNA crosslinks. Reporter activity was determined in RA/DMF-differentiated transfectants. Statistically significant difference in reporter expression with versus without IRF8 knockdown is indicated by $^{*}P < 0.01$ and in IRF8-knockdown cells with versus without reexpression of FANCC, FANCF, or both by $^{**}P < 0.01$ or $^{***}P < 0.01$. Statistically significant differences with IRF8 knockdown and reexpression of FANCC or FANCF versus reexpression of both are indicated by $^{\#}P < 0.01$ or $^{\#\#}P < 0.01$. (**B**) Expression of *Fancc* is decreased in U937 stable transfectants with IRF8 knockdown. U937 stable transfections from the experiments above were analyzed for expression of *Irf8* and *Fancc* mRNA by real-time PCR. Statistically significant differences with versus without IRF8 knockdown are indicated by $^{*}P < 0.01$ and $^{**}P < 0.01$.

between control and IRF8-overexpressing cells (~70% more *Fancc* mRNA in IL-1β– or RA/DMF-treated, IRF8-overexpressing transfectants versus similarly treated control transfectants).

Fancc is an IRF8 target gene. We investigated activation of the *Fancc* promoter by IRF8 using a series of reporter constructs with sequence from the proximal *Fancc* 5′ flank (starting at 1.5 kb relative to the transcription start site). Constructs were designed around potential IRF8-binding sequences (Figure 2A, consensus sequences in red). U937 cells were cotransfected with these promoter/reporter constructs (or empty control vector) and a vector to overexpress IRF8 (or control vector) and analyzed for reporter activity, with or without differentiation. We found that IRF8 overexpression significantly increased activity of constructs with at least 56 bp of *Fancc* promoter sequence but not a construct with 48 bp (Figure 2B). This suggested a possible IRF8-binding cis element between –48 and –56 bp. Consistent with this, the –50 to –56 bp *Fancc* sequence had homology with an IRF-binding consensus (5′-GAAAAT-3′ compared with the ISRE consensus [5′-GAAANN-3′] and the IRF8-binding *Fancf* cis element [5′-GAAAGC-3′]) (17, 33). We mutated this sequence in the context of the –56-bp *Fancc* promoter construct (5′-GAAAAT-3′ to 5′-GAACAT-3′) and found that the mutant construct did not exhibit IRF8-induced promoter activity (Figure 2B).

To test the –50- to –56-bp *Fancc* promoter region for cis element activity, we generated a construct with 3 copies of this *Fancc* sequence linked to a minimal promoter and luciferase reporter gene. This construct (or empty minimal promoter/reporter vector) was cotransfected into U937 cells with an IRF8 expression vector (or empty control vector), and transfectants were analyzed for reporter activity. We found that activity of this *Fancc* cis element was significantly increased by differentiation of the transfectants ($P < 0.001$, $n = 6$) (Figure 2C) and that IRF8 overexpression significantly increased activity of the *Fancc* cis element with or without differentiation ($P < 0.001$, $n = 6$) (Figure 2C). In contrast, activity of a construct with 3 copies of the mutant form of the *Fancc* cis element was not significantly different than empty control reporter vector, with or without IRF8 overexpression or differentiation (data not shown).

To determine whether IRF8 interacted with this *Fancc* cis element, we performed EMSA with a synthetic double-stranded oligonucleotide probe representing the –58- to –46-bp *Fancc* sequence and nuclear proteins from U937 cells. Some binding assays were incubated with excess unlabeled homologous oligonucleotide, homologous oligonucleotide with a mutation of the ISRE-like sequence, or oligonucleotides with 2 irrelevant *Fancc* promoter sequences or the IRF8-binding *FANCF* cis element (17). Other binding assays were preincubated with IRF8 antibody (or control antibody). We found that the –58- to –46-bp *Fancc* sequence bound a specific protein complex, which was disrupted by IRF8 antibody, and had cross-competitive binding with the IRF8-binding *FANCF* cis element but not with mutant or irrelevant *Fancc* sequences (Figure 3A).

We investigated in vivo binding of IRF8 to the *Fancc* promoter by chromatin immunoprecipitation. In vivo cross-linked chromatin from U937 cells was sheared to generate approximately 200-bp fragments, coprecipitated with an IRF8 antibody (or control antibody), and amplified by real-time PCR using primers that flank the *Fancc* cis element or irrelevant sequences from the distal *Fancc* 5’ flank. We found that IRF8 bound specifically to the proximal *Fancc* promoter (Figure 3B). Binding site occupancy by IRF8 was significantly increased by differentiation of U937 cells ($P < 0.0001$, $n = 3$), consistent with transfection data for promoter activity.

Impaired DNA repair in IRF8-deficient myeloid cells is rescued by FANCC. We investigated the contribution of FANCC to impaired

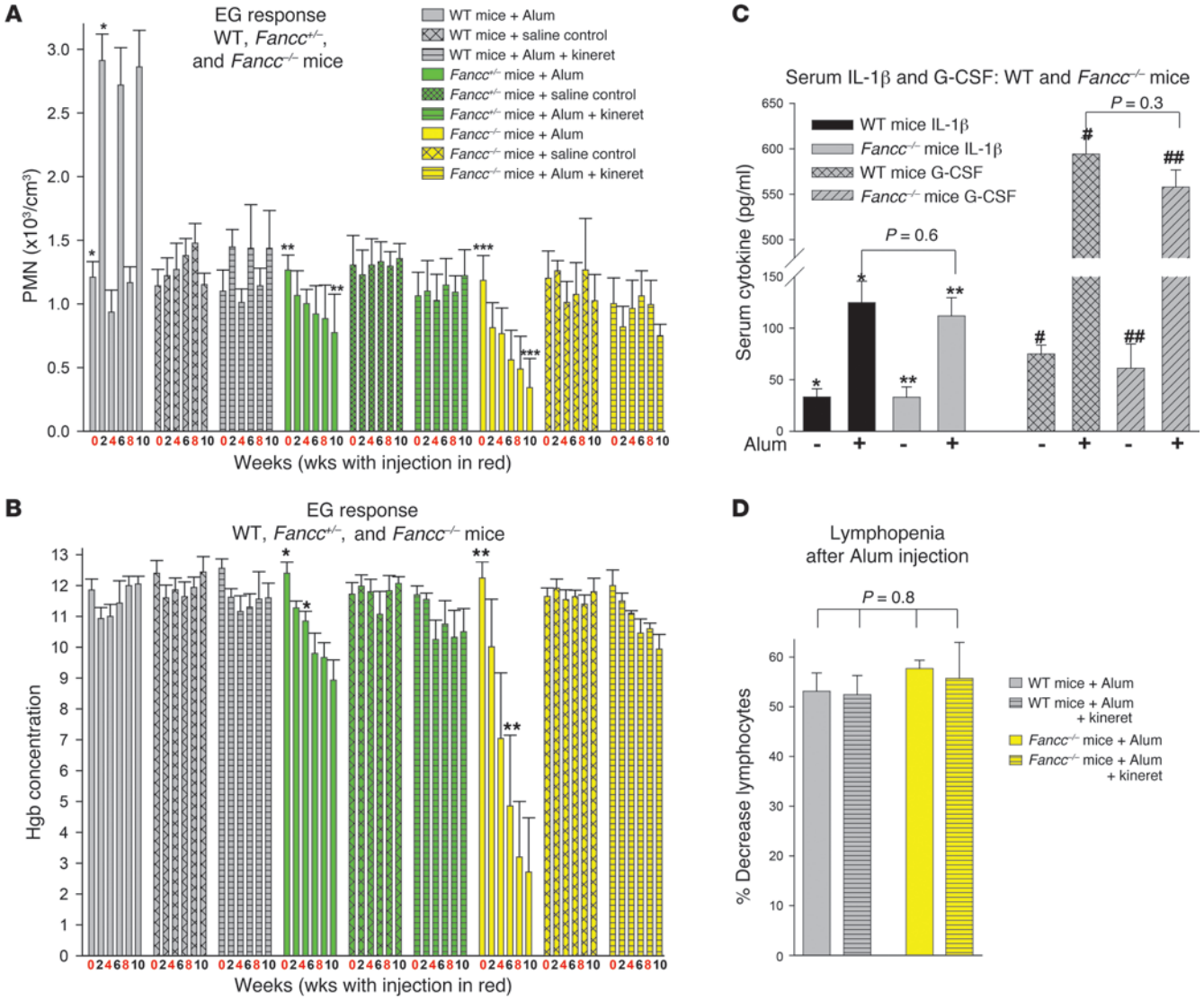

Figure 5

FANCC-deficient mice exhibit an abnormal emergency granulopoiesis response. (**A**) *Fancc*$^{+/-}$ and *Fancc*$^{-/-}$ mice fail to exhibit granulocytosis upon Alum injection. WT, *Fancc*$^{+/-}$, and *Fancc*$^{-/-}$ mice were injected with saline or Alum in the peritoneal cavity every 4 weeks. Some mice were pretreated with IL-1R antagonist (anakinra [Kineret]) 24 hours prior to and following Alum injection. Peripheral blood granulocyte counts were determined every 2 weeks. Statistically significant differences that developed over time are indicated by $^{*}P < 0.01$, $^{**}P < 0.01$, or $^{***}P < 0.01$. (**B**) FANCC-deficient mice exhibit progressive anemia with repeated Alum injection. Mice described above were also evaluated for Hgb concentration every 2 weeks. Statistically significant differences that developed over time are indicated by $^{*}P < 0.01$ and $^{**}P < 0.01$. (**C**) IL-1β and G-CSF production are similar in Alum-injected WT and *Fancc*$^{-/-}$ mice. Serum levels of IL-1β and G-CSF were determined in WT or *Fancc*$^{-/-}$ mice injected with Alum or saline. Statistically significant differences with versus without Alum are indicated by $^{*}P < 0.01$, $^{**}P < 0.01$, $^{\#}P < 0.01$, or $^{\#\#}P < 0.01$. (**D**) Lymphopenia occurs in WT and *Fancc*$^{-/-}$ mice after Alum injection. The percentage decrease in lymphocyte counts after Alum injection were determined in WT and *Fancc*$^{-/-}$ mice, with versus without anakinra pretreatment. Lymphocyte counts were not altered by saline injection (data not shown). EG, emergency granulopoiesis.

DNA repair in IRF8-deficient cells using a reporter-based repair assay. In these studies, the reporter plasmid is treated with mitomycin C (MMC) to generate DNA crosslinks prior to transfection into U937 cells (a TK-luciferase plasmid for the current studies) (17). Decreased reporter activity from MMC-treated plasmid versus untreated plasmid reflects MMC-induced DNA damage in this assay (17). Therefore, conditions that increase reporter activity in cells transfected with MMC-treated plasmid (but not control plasmid) are presumed to increase the efficiency of DNA repair.

We found that reporter activity of MMC-treated plasmid in U937 transfectants was significantly less than that of control plasmid, consistent with our previous studies (17). As in those studies, the difference in reporter activity with versus that without MMC treatment was greater in differentiating transfectants ($P < 0.001$, $n = 3$). We also found that expression of IRF8-specific shRNAs significantly decreased activity of MMC-treated reporter plasmid ($P < 0.01$, $n = 3$) but not untreated, control plasmid ($P = 0.1$, $n = 3$) (Figure 4A). We found that reexpression of either FANCC or

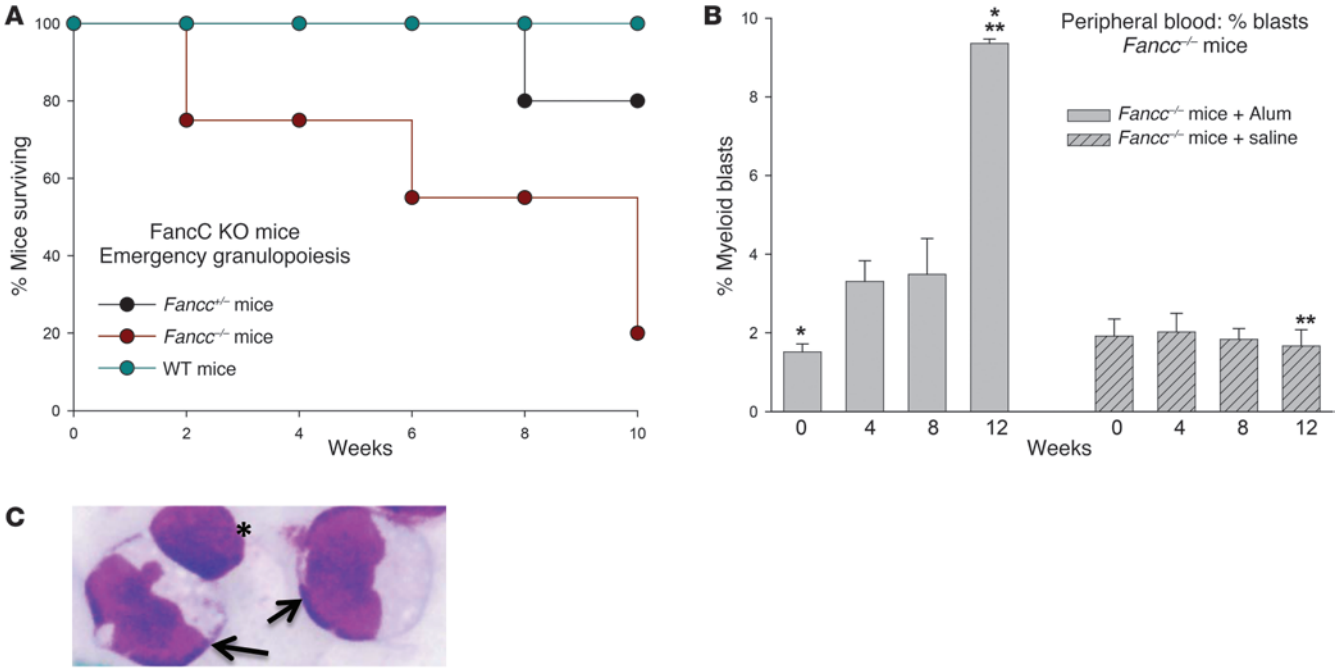

Figure 6

Abnormal myelopoiesis develops in *Fancc*$^{-/-}$ mice after multiple cycles of Alum injection. (**A**) Survival of *Fancc*$^{-/-}$ mice is low during multiple cycles of Alum injection. *Fancc*$^{-/-}$, *Fancc*$^{+/-}$, and WT mice were injected with Alum or saline every 4 weeks. The percentage of mice surviving during the treatment period was determined. All mice in the saline group survived during the treatment period. Curves for WT and *Fancc*$^{-/-}$ mice were significantly ($P < 0.01$) different by log-rank analysis. (**B**) Immature myeloid cells appear in the circulation of *Fancc*$^{-/-}$ mice after multiple Alum injections. Peripheral blood from the mice above was analyzed every 4 weeks for immature circulating myeloid cells (blasts). Statistically significant difference in myeloid blasts over time in Alum-injected mice is indicated by $*P < 0.01$ and with versus without Alum injection by $**P < 0.01$. No myeloid blasts were observed in WT or *Fancc*$^{+/-}$ mice during treatment. (**C**) Photomicrograph of immature myeloid cells in the circulation of *Fancc*$^{-/-}$ mice. Peripheral blood from a *Fancc*$^{-/-}$ mouse after 2 Alum injection cycles was analyzed microscopically (original magnification, ×40). Myeloid blasts are indicated by arrows, and a lymphocyte is indicated by an asterisk.

FANCF in transfectants with IRF8 knockdown significantly increased activity from MMC-treated reporter plasmid ($P < 0.02$, $n = 3$) (Figure 4A). The effect of coexpressing FANCC and FANCF on MMC-treated reporter plasmid activity in cells with IRF8 knockdown was greater than the effect of either alone ($P = 0.03$, $n = 3$).

In control studies, preliminary transfections were performed to identify the maximal amount of FANCC or FANCF expression vector that did not influence activity of the MMC-treated reporter construct in the absence of IRF8 knockdown (data not shown). The identified amount was used in these studies, because the goal was to study effects of expressing FANCC or FANCF specifically on IRF8-induced defects on DNA repair (as opposed to other abnormalities in U937 cells). Neither overexpression of FANCC or FANCF, nor knockdown of IRF8 influenced reporter activity from non-MMC-treated control reporter plasmid. U937 cells that were stably expressing IRF8-specific shRNAs were used for these studies. In other control studies, we found that expression of *Fancc* mRNA was decreased by IRF8 knockdown, as anticipated (Figure 4B). We previously demonstrated that IRF8 knockdown decreased *Fancf* mRNA and protein (17).

These studies suggested that decreased expression of FANCC contributes to impaired DNA repair in IRF8-deficient cells. Because of the involvement of IRF8 in the innate immune response, we hypothesized that Fanconi pathway activity might be a required for successful emergency granulopoiesis.

The emergency granulopoiesis response is impaired in FANCC-deficient mice. Bone marrow from *Fancc*$^{-/-}$ mice has increased susceptibility to MMC-induced DNA damage in vitro and in vivo. These mice do not develop bone marrow failure, dysplasia, or AML in the absence of a DNA-damaging event (34–37), but emergency granulopoiesis has not been investigated in any FA mice. Emergency granulopoiesis is studied in mice by i.p. injection with pathogens or antigen/adjuvant combination (ovalbumin/alum, referred to as Alum) (38). In both models, there is an increase in IL-1β and in IL-1β–dependent production of G-CSF (38–41). Pathogen-based studies are characterized by death of the animals, but mice recover completely from Alum injection. Since we were interested in studying multiple episodes of emergency granulopoiesis, we chose the latter approach.

In preliminary studies with WT mice, we determined that peripheral granulocytosis was maximal 2 weeks after Alum injection and resolved by 4 weeks (Figure 5A). We identified mild anemia in these mice during the first 2 cycles of Alum injection, which resolved with subsequent treatment (Figure 5B). Based on these results, we embarked on an every-4-week injection program. We injected Alum or saline control (10 mice per group) into the peritoneal cavity of WT, *Fancc*$^{+/-}$, and *Fancc*$^{-/-}$ mice on day 0, and complete blood counts were performed every 2 weeks. We found that Alum injection did not induce granulocytosis in *Fancc*$^{+/-}$ or *Fancc*$^{-/-}$ mice at 2 weeks (Figure 5A). Instead, FANCC-knockout mice developed progressive granulocytopenia with repeated cycles

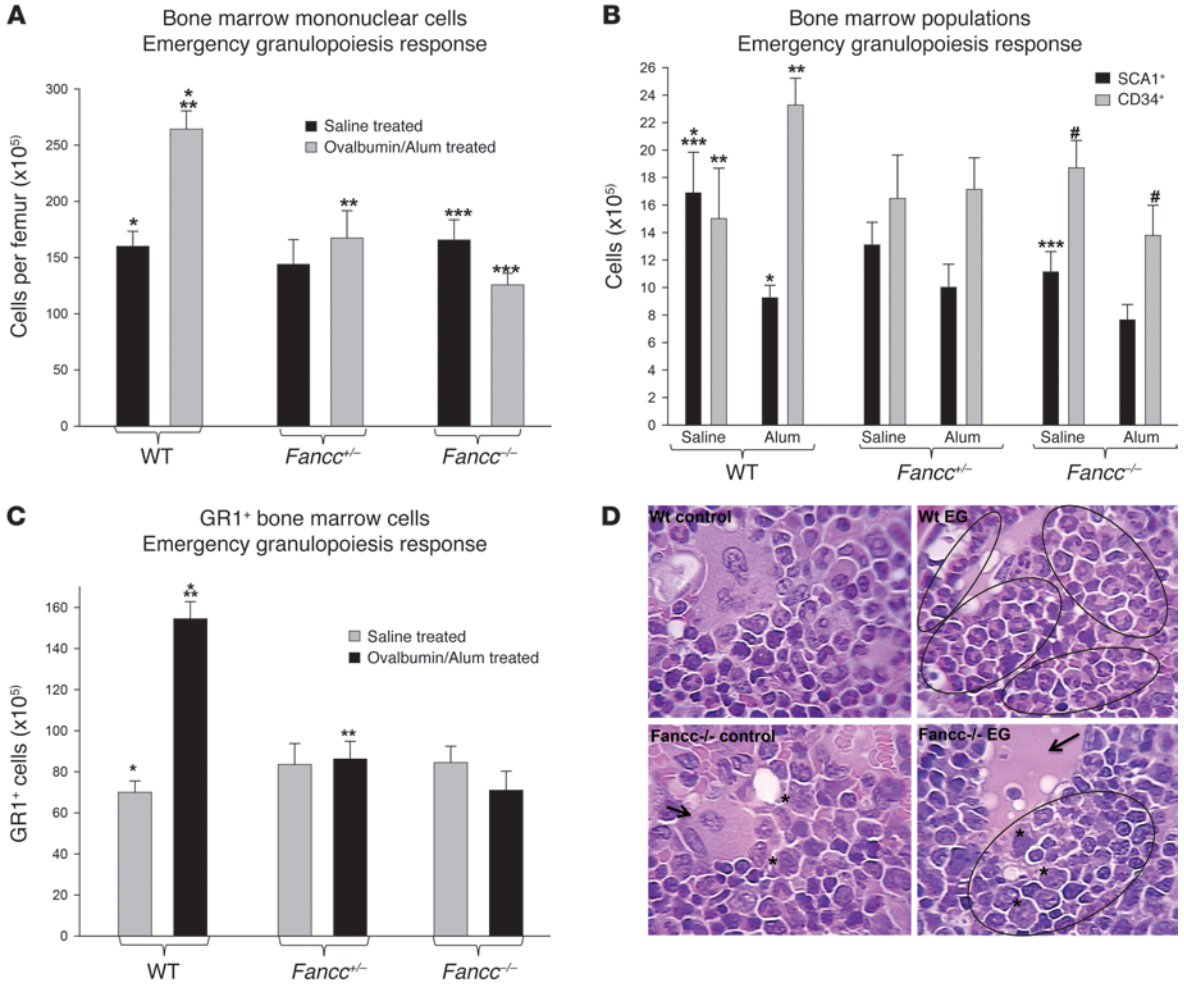

Figure 7

Alum injection does not expand myeloid progenitors or differentiating granulocytes in *Fancc*$^{-/-}$ mice. (**A**) Alum increases total bone marrow cells in WT but not FANCC-deficient mice. WT, *Fancc*$^{+/-}$, and *Fancc*$^{-/-}$ mice were injected with Alum or saline. Bone marrow was harvested 2 weeks later, and total bone marrow mononuclear cells were counted. Statistically significant differences with versus without Alum are indicated by $^{*}P < 0.01$ or $^{***}P < 0.01$ and with versus without FANCC-knockout by $^{**}P < 0.01$. (**B**) Alum decreases SCA1^{+} cells and increases CD34^{+} in WT, but not FANCC-deficient, mice. Bone marrow from the mice above was analyzed by flow cytometry for immature (SCA1^{+}CD34^{-}) or committed myeloid progenitors (SCA1^{-}CD34^{+}GR1^{-}). Statistically significant differences with versus without Alum are indicated by $^{*}P < 0.01$, $^{**}P < 0.01$, or $^{\#}P < 0.01$ and with versus without FANCC-knockout by $^{***}P < 0.01$. (**C**) Alum increases differentiating granulocytes in the bone marrow of WT mice but not FANCC-deficient mice. The bone marrow above was analyzed for differentiating myeloid progenitors (CD34^{-}GR1^{+}). Statistically significant differences with versus without Alum are indicated by $^{*}P < 0.01$ and with versus without FANCC-knockout by $^{**}P < 0.01$. (**D**) Bone marrow from FANCC-deficient mice is abnormal. Sternal bone marrow from mice above was examined microscopically (original magnification, ×40). Areas of differentiating granulocytes in WT bone marrow after Alum are encircled. A dysplastic megakaryocyte in control *Fancc*$^{-/-}$ bone marrow is indicated by an arrow, and hypersegmented granulocytes are indicated by asterisks. Hyaline debris in *Fancc*$^{-/-}$ bone marrow from Alum-treated mice is indicated by an arrow, areas of degrading cells are encircled, and abnormal granulocyte progenitors are indicated by asterisks.

of Alum injection. This effect was profound in *Fancc*$^{-/-}$ mice and significantly less in *Fancc*$^{+/-}$ mice ($P < 0.01$, $n = 8$). We found that FANCC-knockout mice developed progressive anemia with successive cycles of Alum injection (Figure 5B). Anemia was severe in *Fancc*$^{-/-}$ mice and was the likely cause of death in these animals.

We performed control studies to verify that Alum injection had an equivalent influence on circulating levels of IL-1β and G-CSF in WT and *Fancc*$^{-/-}$ mice. In initial studies, we found that the concentration of these cytokines was maximal 4 days after injection in either WT or *Fancc*$^{-/-}$ mice (data not shown). We found that Alum injection significantly increased the serum concentrations of both IL-1β and G-CSF in WT and *Fancc*$^{-/-}$ mice ($P < 0.001$, $n = 3$) (Figure 5C). The concentrations of these cytokines were not significantly different in Alum-treated WT versus *Fancc*$^{-/-}$ mice ($P = 0.6$ for IL-1β and $P = 0.3$ for G-CSF; $n = 3$).

Injection with Alum also results in lymphopenia in these mice, which is maximal at 24 to 48 hours. A number of cytokines were examined by other investigators to identify a mechanism for this observation, and increased TNF-α was found to be the cause of lymphopenia in this murine model (41). We observed an equivalent TNF-α effect on circulating lymphocytes in WT and *Fancc*$^{-/-}$ mice (decrease of 53.1% ± 3.6% in WT mice and 57.7% ± 1.6% in *Fancc*$^{-/-}$ mice; $P = 0.4$, $n = 4$) (Figure 5D).

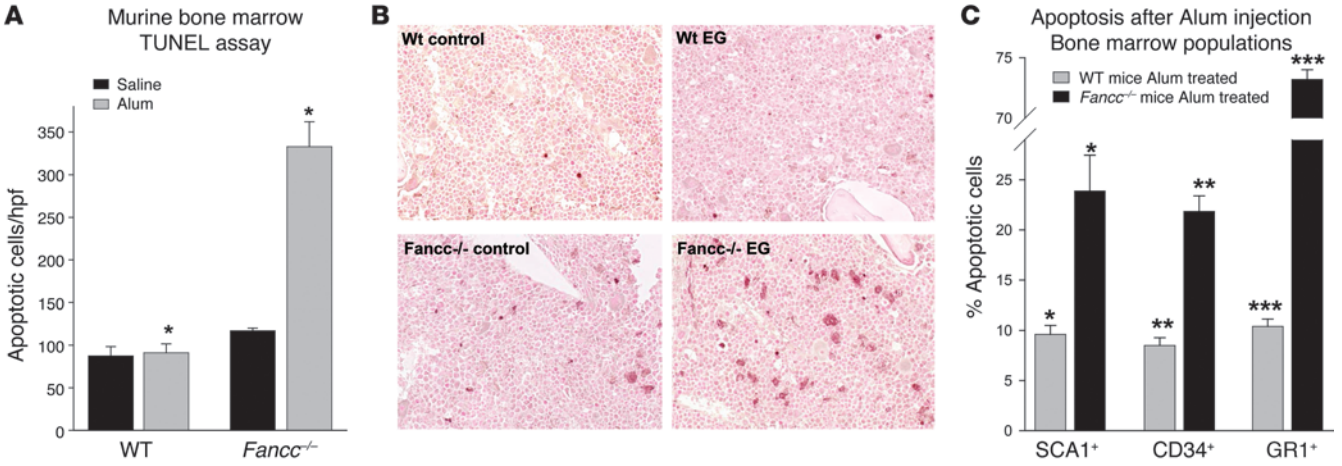

Figure 8

Alum injection induces apoptosis in the bone marrow of FANCC-deficient mice. (**A**) Alum injection increases apoptosis in the bone marrow of FANCC-deficient, but not WT, mice. TUNEL assays were performed on sternal bone marrow from WT and *Fancc*$^{-/-}$ mice 2 weeks after i.p. injection with Alum or saline. Positive cells were counted per high-power field (hpf). Statistically significant differences in cell numbers in WT versus *Fancc*$^{-/-}$ bone marrow are indicated by $^{*}P < 0.01$. (**B**) Bone marrow from FANCC-deficient mice has increased apoptosis by TUNEL assay. Photomicrographs (original magnification, ×40) were obtained from the sternal bone marrow samples, described above. (**C**) Hematopoietic stem and myeloid progenitor cells are apoptotic in the bone marrow of Alum-injected *Fancc*$^{-/-}$ mice. Bone marrow from WT or *Fancc*$^{-/-}$ mice was harvested 2 weeks after injection with Alum or saline and analyzed by flow cytometry to identify the percentage of Annexin V–positive cells in the SCA1^{+}, CD34^{+}, or GR1^{+} populations. Statistically significant differences in the percentages of Annexin V–positive cells in WT versus *Fancc*$^{-/-}$ bone marrow populations are indicated by $^{*}P < 0.01$, $^{**}P < 0.01$, or $^{***}P < 0.01$.

Fancc$^{-/-}$ mice exhibited significant ($P < 0.001$) mortality with multiple cycles of Alum injection in comparison with that of WT mice (80% of mice did not survive the treatment period) (Figure 6A). In contrast, 80% of *Fancc*$^{+/-}$ and 100% of WT Alum-injected mice survived the treatment period. There were no deaths among the saline-injected cohorts of WT, *Fancc*$^{+/-}$, or *Fancc*$^{-/-}$ mice. In the few *Fancc*$^{-/-}$ mice that did not succumb during repeated cycles of Alum injection, increasing numbers of myeloid blasts appeared in the circulation (Figure 6, B and C). However, no myeloid blasts were found in the circulation of WT or *Fancc*$^{+/-}$ mice, even after 4 cycles of Alum injection, and no saline-injected mice of any type exhibited circulating myeloid blasts during the course of the experiment.

In additional control studies, we investigated IRF8 expression in *Fancc*$^{-/-}$ murine bone marrow. For these studies, cells from WT or *Fancc*$^{-/-}$ mice were cultured under GMP conditions, and expression of IRF8 was determined by real-time PCR, with or without IL-1β treatment. We found no significant difference in IRF8 expression in WT versus *Fancc*$^{-/-}$ cells under either condition ($P > 0.2$, $n = 3$).

IL-1R blockade protects Fancc$^{-/-}$ *mice during emergency granulopoiesis*. Since IL-1β is a key mediator of emergency granulopoiesis, we investigated the effect of IL-1R blockade on the consequences of Alum injection in FANCC-knockout mice. For these studies, we used an IL-1R antagonist that is in use in for human autoimmune disease (anakinra [Kineret]) (42, 43). WT, *Fancc*$^{+/-}$, and *Fancc*$^{-/-}$ mice were pretreated with anakinra 24 hours before Alum injection and an additional dose was given 24 hours later (10 mice per group). We found that anakinra blocked granulocytosis in Alum-treated WT mice, as anticipated ($P < 0.001$ for maximal granulocytes) (Figure 5A). WT mice treated with the Alum-anakinra combination also did not exhibit anemia during the initial treatment period (Figure 5B). Mortality of WT mice was not increased by IL-1R antagonist treatment, with or without Alum injection.

We found that pretreatment with IL-1R antagonist prevented granulocytopenia in Alum-treated *Fancc*$^{+/-}$ and *Fancc*$^{-/-}$ mice (Figure 5A). IL-1R blockade also significantly decreased the development of anemia in *Fancc*$^{-/-}$ mice during multiple cycles of Alum injection (Figure 5B). Perhaps more importantly, none of the anakinra-treated *Fancc*$^{+/-}$ or *Fancc*$^{-/-}$ mice died during 3 cycles of Alum treatment.

Since IL-1R blockade would not be expected to influence TNF-α in this model, we investigated the effect of anakinra on lymphocyte counts in these mice, as above. Consistent with the specificity of this agent for the IL-1R, we found that lymphopenia occurred in Alum-injected, anakinra-treated WT and *Fancc*$^{-/-}$ mice (decrease of 54.4% ± 3.8% in WT mice and 55.7% ± 7.2% in *Fancc*$^{-/-}$ mice; $P = 0.6$, $n = 4$) (Figure 5D). These values were not significantly different than the lymphopenia seen in Alum-treated mice in the absence of anakinra ($P = 0.8$, $n = 4$).

Apoptosis in Fancc$^{-/-}$ *bone marrow during failed emergency granulopoiesis*. We investigated the effect of Alum injection on various cell populations in the bone marrow of WT and FANCC-knockout mice. For these studies, WT, *Fancc*$^{+/-}$, or *Fancc*$^{-/-}$ mice were treated with a single i.p. injection of Alum or saline and sacrificed 2 weeks later. We found that the total number of bone marrow mononuclear cells increased significantly after injection of Alum in WT mice but not *Fancc*$^{+/-}$ or *Fancc*$^{-/-}$ mice (Figure 7A). In fact, the total number of bone marrow mononuclear cells in *Fancc*$^{-/-}$ mice actually decreased after Alum injection.

We used flow cytometry to identify populations of immature progenitors (SCA1^{+}CD34^{-}GR1^{-}), committed progenitors (SCA1^{-}CD34^{+}GR1^{-}), or differentiating phagocytes (SCA1^{-}CD34^{-}GR1^{+}) in the bone marrow of these mice. In WT mice, Alum injection decreased the SCA1^{+} population and increased the CD34^{+} (Figure 7B) and GR1^{+} populations (Figure 7C) ($P < 0.02$, $n = 4$), consistent with the physiology of emergency granulopoiesis.

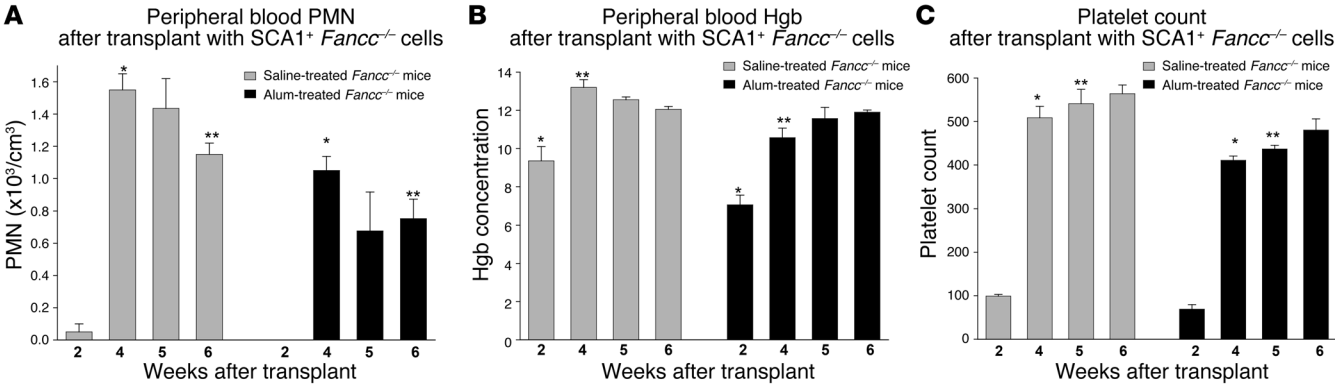

Figure 9

Hematopoietic recovery is delayed in mice transplanted with SCA1+ cells from Alum-treated *Fancc*$^{-/-}$ mice versus control *Fancc*$^{-/-}$ mice. (**A**) Circulating neutrophils increase more slowly in mice transplanted with SCA1+ bone marrow cells from Alum-treated versus control *Fancc*$^{-/-}$ mice. *Fancc*$^{-/-}$ mice were injected with Alum or saline, and bone marrow was harvested 2 weeks later. LIN$^-$SCA1+ cells were transplanted into lethally irradiated WT mice, and peripheral neutrophil counts were determined each week. Statistically significant differences with transplant from Alum- versus saline-treated donors is indicated by $^*P < 0.01$ or $^{**}P < 0.01$. (**B**) Hgb concentration increases more slowly in mice transplanted with SCA1+ bone marrow cells from Alum-treated versus control *Fancc*$^{-/-}$ mice. Hgb concentrations were determined for the mice above. Statistically significant differences with transplant from Alum- versus saline-injected donors are indicated by $^*P < 0.01$ or $^{**}P < 0.01$. (**C**) Platelet counts increase more slowly in mice transplanted with SCA1+ bone marrow cells from Alum-treated versus control *Fancc*$^{-/-}$ mice. Platelet counts were determined for the mice above. Statistically significant differences with transplant from Alum- versus saline-injected donors are indicated by $^*P < 0.01$ or $^{**}P < 0.01$.

In contrast, Alum injection did not increase CD34$^+$ cells in *Fancc*$^{+/-}$ mice and actually decreased the number of CD34$^+$ cells in *Fancc*$^{-/-}$ mice (Figure 7B). Alum treatment also did not increase the number of GR1$^+$ cells in *Fancc*$^{+/-}$ or *Fancc*$^{-/-}$ murine bone marrow (Figure 7C).

Histological examination of hematoxylin and eosin–stained sternal bone marrow from these mice was performed to confirm these results. We found that WT murine bone marrow was filled with maturing neutrophils 2 weeks after Alum injection, as anticipated (Figure 7D). In contrast, Alum injection did not increase the abundance of mature granulocytes in *Fancc*$^{-/-}$ bone marrow (Figure 7D). Instead, an increase in cells with pyknotic nuclei, enlarged myeloid progenitor cells with disrupted nuclei, and areas of cellular debris were observed. There were many areas of hyalinized material in *Fancc*$^{-/-}$ bone marrow after Alum treatment, suggestive of organizing cellular debris. In non-Alum-injected *Fancc*$^{-/-}$ bone marrow, we noted mononucleate megakaryocytes and hypersegmented neutrophils, indicating mild bone marrow dysplasia at baseline in these mice.

To determine whether apoptosis of bone marrow cells contributed to failed emergency granulopoiesis in *Fancc*$^{-/-}$ mice, we performed TUNEL assays on sternal bone marrow from WT or *Fancc*$^{-/-}$ mice 2 weeks after Alum injection. We found a significant increase in the number of TUNEL-positive cells in Alum-treated *Fancc*$^{-/-}$ mice in comparison with that in Alum-treated WT mice or saline-treated WT or *Fancc*$^{-/-}$ mice (analyzed per high-power field; Figure 8A). This increase was more pronounced than the absolute number indicates, because the number of bone marrow cells per high-power field in Alum-treated WT mice was significantly greater than that in Alum-treated *Fancc*$^{-/-}$ mice (see Figure 7A). Visual inspection of sternal bone marrow samples from Alum-treated *Fancc*$^{-/-}$ mice revealed clusters of apoptotic cells that were not apparent in saline-injected *Fancc*$^{-/-}$ mice or WT mice under either condition (Figure 8B).

We further analyzed bone marrow from Alum-injected mice to identify cell populations that were undergoing apoptosis. For these studies, bone marrow was obtained from WT or *Fancc*$^{-/-}$ mice 2 weeks after Alum injection and analyzed by flow cytometry for surface marker expression and Annexin V staining. We found that the percentage of apoptotic SCA1$^+$, CD34$^+$, and GR1$^+$ cells in the bone marrow of Alum-treated *Fancc*$^{-/-}$ mice was greater than that in WT mice (respectively, $P = 0.01$, $P = 0.04$, $P = 0.001$; $n = 3$) (Figure 8C). These differences were likely greater than calculated, based on the decreased number of CD34$^+$ and GR1$^+$ cells in *Fancc*$^{-/-}$ bone marrow versus the increased number of these cells in WT mice after Alum treatment (i.e., there were likely more dead cells discarded during processing or analysis of *Fancc*$^{-/-}$ bone marrow).

Function of bone marrow progenitors from Alum-treated Fancc$^{-/-}$ *mice.* We hypothesized that failed episodes of emergency granulopoiesis resulted in damage to HSCs and bone marrow progenitor cells. We investigated this in bone marrow transplantation experiments. For these studies, bone marrow was harvested from *Fancc*$^{-/-}$ mice 2 weeks after injection with Alum or saline. LIN$^-$SCA1$^+$ cells were isolated and transplanted into lethally irradiated WT mice (5×10^5 cells, after depletion of Annexin V$^+$ cells; cells were ~90% SCA1$^+$ by flow cytometry). Mice were followed with weekly peripheral blood counts. We found that reconstitution of hematopoiesis was significantly delayed in mice that were transplanted with SCA1$^+$ cells from Alum-treated *Fancc*$^{-/-}$ mice in comparison with transplantation with the same number of SCA1$^+$ cells from saline-injected *Fancc*$^{-/-}$ mice. This was reflected in significantly fewer circulating neutrophils ($P < 0.02$, $n = 3$) (Figure 9A), decreased hemoglobin (Hgb) concentration ($P < 0.001$, $n = 3$) (Figure 9B), and a reduced number of circulating platelets ($P < 0.01$, $n = 3$) (Figure 9C).

Bone marrow was obtained from these mice 6 weeks after transplantation for further analysis. We found that the number of bone marrow mononuclear cells was significantly lower in mice transplanted with SCA1$^+$ cells from Alum-treated *Fancc*$^{-/-}$ mice in comparison with that in saline-treated *Fancc*$^{-/-}$ mice ($P = 0.004$, $n = 3$) (Figure 10A). The number of LIN$^-$SCA1$^+$ cells was also significantly lower in the mice transplanted with cells from Alum-treated versus saline-treated *Fancc*$^{-/-}$ mice ($P = 0.007$, $n = 3$) (Figure 10B). To confirm that these SCA1$^+$ cells originated

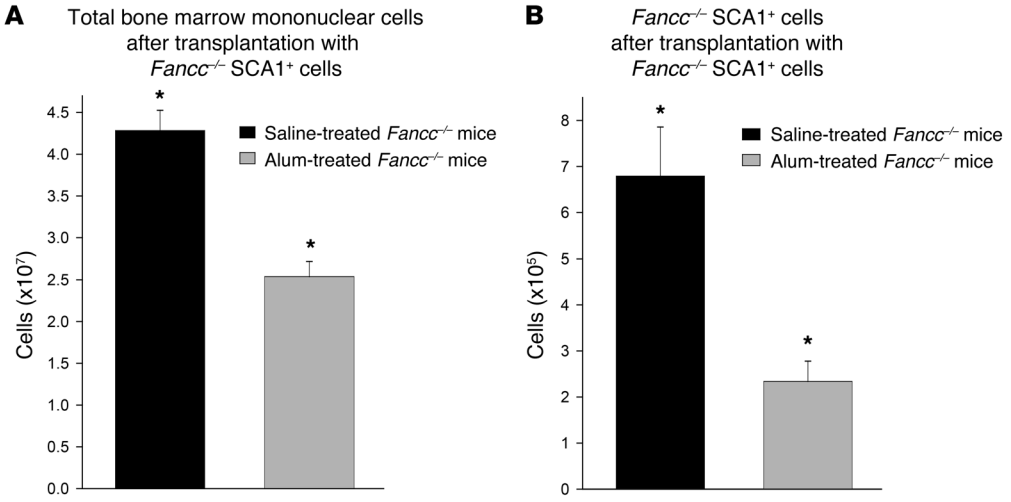

Figure 10
Fewer SCA1+ cells are found in the bone marrow after transplantation with SCA1+ cells from Alum-treated *Fancc*$^{-/-}$ mice versus saline-treated *Fancc*$^{-/-}$ mice. (**A**) Fewer bone marrow mononuclear cells are present in mice transplanted with SCA1+ cells from Alum-injected *Fancc*$^{-/-}$ mice versus saline-injected *Fancc*$^{-/-}$ mice. *Fancc*$^{-/-}$ mice were injected with Alum or saline i.p., and bone marrow was harvested 2 weeks later. LIN$^-$SCA1+ cells were transplanted into irradiated WT recipients. Bone marrow was harvested 6 weeks after transplantation, and total bone marrow mononuclear cells were counted. Statistically significant difference between cell numbers after transplantation with cells from Alum-treated versus control *Fancc*$^{-/-}$ mice is indicated by $^*P < 0.01$. (**B**) Fewer SCA1+ cells are present in mice transplanted with SCA1+ cells from Alum-treated *Fancc*$^{-/-}$ mice versus saline-treated *Fancc*$^{-/-}$ mice. Bone marrow cells above were analyzed by flow cytometry for SCA1+ cells. Statistically significant differences between cell numbers after transplantation with cells from Alum-treated versus control *Fancc*$^{-/-}$ mice are indicated by $^*P < 0.01$.

from the *Fancc*$^{-/-}$ transplanted population, we analyzed genomic DNA from LIN$^-$SCA1+ cells for the presence of the antibiotic resistance cassette used to generate the *FANCC* knockout (by real-time PCR). An irrelevant gene (*ARIH2*) was used as a control for total genomic DNA in the sample. We found that most SCA1+ cells present in the bone marrow of these mice 6 weeks after transplantation were *Fancc*$^{-/-}$ cells (92.0% ± 8.1% for recipients of bone marrow from non-Alum-treated donors and 91.3% ± 5.8% for Alum-treated donors recipients; $P = 0.9$, $n = 3$).

Discussion

We found that treatment of myeloid progenitor cells with emergency granulopoiesis–related cytokines (IL-1β and G-CSF) resulted in IRF8-dependent transcription of the gene encoding FANCC. We also found an abnormal response to emergency granulopoiesis challenge in FANCC-deficient mice. Specifically, *Fancc*$^{-/-}$ mice failed to exhibit granulocytosis but instead had progressive neutropenia and anemia with repeated challenge. This failure of the emergency granulopoiesis response was associated with apoptosis of bone marrow HSCs and differentiating myeloid progenitors. *Fancc*$^{-/-}$ mice that survived 3 cycles of attempted emergency granulopoiesis exhibited a new onset of leukocytosis with immature myeloid cells. Therefore, our studies suggested that FANCC was an essential component of the emergency granulopoiesis response and provided a previously undescribed mechanism for bone marrow failure in FA.

IRF8 plays a role in the innate immune response by regulating a set of phagocyte effector genes, including genes encoding the rate-limiting phagocyte NADPH-oxidase proteins (2, 3). In the current studies, we identified transcriptional activation of *FANCC* by IRF8 as an additional component of the innate immune response. Our studies suggest that FANCC expression contributes to Fanconi pathway activation during infectious challenge. Fanconi core components are a logical control point for pathway activity, since assembly and DNA localization of the core complex leads to ubiquitination of FANCD2 and FANCI, a process that initiates DNA repair.

We found enrichment of FANCC in the chromatin fraction of murine myeloid progenitor cells upon treatment with IL-1β. This was consistent with our hypothesis regarding Fanconi pathway activation during emergency granulopoiesis. We found that FANCJ and RAD51 were also enriched in the chromatin fraction in IL-1β–treated cells. RAD51 is associated with the HRR DNA repair mechanism, and FANCJ participates in both HRR and TLS (18–20). Both mechanisms contribute to replication fork recovery, so this data is also consistent with our hypothesis. Studies are ongoing in the laboratory to clarify DNA repair mechanisms that are activated during emergency granulopoiesis

We hypothesized that impaired Fanconi pathway activity in IRF8-deficient mice accelerates accumulation of mutations during the stress of emergency granulopoiesis, contributing to development of AML. This was consistent with observations that *Irf8*$^{-/-}$ mice do not exhibit emergency granulopoiesis, but repeated infectious challenge accelerates progression to AML in these mice (our unpublished observations). To investigate this further, we tested a murine FA model for integrity of the emergency granulopoiesis response. We found that *Fancc*$^{-/-}$ mice did not exhibit leukocytosis in response to emergency granulopoiesis stimuli but instead developed progressive neutropenia, profound anemia, and death. The few *Fancc*$^{-/-}$ mice that survived 3 cycles of emergency granulopoiesis developed leukocytosis with immature cells. This was similar to human subjects who survive the bone marrow failure phase of FA.

Fancc$^{+/-}$ mice also had an impaired granulocytosis response and developed mild anemia. These results suggested that human subjects with heterozygous Fanconi deficiency may also have an impaired emergency granulopoiesis response. This would not be anticipated

to result in a profound phenotype in these individuals, since studies have shown that as little as 10% normal neutrophil function can protect from recurrent infection (44). However, study of FA carriers, and their clinical responses to infection, might be of interest.

In normal bone marrow, IL-1β induces proliferation of HSCs and committed myeloid progenitor cells during the emergency granulopoiesis response, associated with S-phase shortening. In contrast, we found increased apoptosis of HSCs and differentiating myeloid progenitor cells in the bone marrow of *Fancc*$^{-/-}$ mice after emergency granulopoiesis stimuli. Indeed, the majority of differentiating myeloid progenitor cells were apoptotic, consistent with an absence of granulocytosis in the bone marrow or circulation in Alum-treated *Fancc*$^{-/-}$ mice. We also found HSC dysfunction in *Fancc*$^{-/-}$ mice after even a single cycle of in vivo stimulation with Alum. These results support our hypothesis that failed episodes of emergency granulopoiesis contribute to bone marrow failure in FA.

In *Fancc*$^{-/-}$ mice, profound anemia was common after 2 cycles of Alum stimulation. Since IL-1β suppresses erythroid progenitor proliferation, IL-1β–induced suppression followed by an unsuccessful compensatory proliferation of erythroid progenitors may contribute to progressive anemia in our studies. The inflammatory mediators IFN-γ and TNF-α have a greater proapoptotic effect in FANCC-deficient bone marrow in comparison with that in normal bone marrow (45, 46). Mutations that reverse the susceptibility of *Fancc*$^{-/-}$ cells to cytokine-induced programmed cell death may contribute to clonal progression in FA. These are topics for future studies.

Additionally, these inflammatory cytokines may impact bone marrow failure during the emergency granulopoiesis response. Previous investigators determined that Alum injection does not increase IFN-γ levels, but production of TNF-α is increased in these mice (41, 47). Therefore, we considered the possibility that TNF-α influenced apoptosis of bone marrow cells in our studies. Other investigators determined that TNF-α production is maximal 24–48 hours after Alum injection (41). In elegant studies, these investigators also demonstrated that increased TNF-α is directly causal of lymphopenia observed in these mice 24–48 hours after Alum injection (41). We confirmed these results in studies, as described above (and in data not shown). Since TNF-α production is not dependent upon increased IL-1β in Alum-injected mice (which occurs later), pretreatment with an IL-1R antagonist would not be anticipated to influence effects of TNF-α on these mice (41). Consistent with this, we found that lymphopenia occurred equivalently after Alum injection in WT and *Fancc*$^{-/-}$ mice, with or without anakinra pretreatment. These results suggested the possibility that blocking TNF-α might add to anakinra effects and further protect HSCs and progenitor cells from apoptosis during emergency granulopoiesis in *Fancc*$^{-/-}$ mice. This will be a topic for future investigations.

It is of interest that IL-1β is increased in human subjects with FA (48). This may imply subclinical, ongoing infection in subjects with FA, resulting in chronic production of this cytokine. Our current studies suggest that such subclinical infections may produce ongoing bone marrow stress. In this case, treatment with prophylactic antibiotics might be useful in human subjects with FA. We tested IL-1R blockade as an approach to protecting *Fancc*$^{-/-}$ mice from bone marrow failure during repeated emergency granulopoiesis challenge. We used an IL-1R antagonist (anakinra) that is FDA approved for human subjects with autoimmune disorders and has been previously used in murine models (43, 49). We found that treatment with anakinra blocked emergency granulopoiesis in WT mice and ameliorated bone marrow failure in Alum-treated FANCC-knockout mice. Our studies imply a potential benefit to IL-1R blockade or prophylactic antibiotics to prevent or delay these adverse consequences in human subjects with FA.

Methods

Plasmids

Protein expression vectors. The IRF8 cDNA was obtained from Ben Zion-Levi (Technion, Haifa, Israel) and subcloned into the pcDNAamp mammalian expression vector (Stratagene). The FANCC cDNA was obtained from U937 cells by reverse transcription and real-time PCR. The PCR product was sequenced to assure that no mutations were present. IRF8-specific shRNAs were designed and subcloned into the pLKO expression vector, as previously described (15, 16). These shRNAs consistently reduce IRF8 expression in U937 cells by 70% (15, 16).

Fancc reporter vectors. 5′ flank *Fancc* gene sequences were obtained from U937 genomic DNA by PCR. Fragments were sequenced on both strands to verify identity with reported sequences. Constructs were generated with the pGL3-basic vector (Promega) using 1.5 kb, 1.0 kb, 440 bp, 152 bp, 56 bp, and 48 bp of *Fancc* 5′ flank.

Other reporter constructs were generated with an artificial promoter/reporter vector with 3 copies of an IRF8-binding cis element from the *Fancc* promoter (–58 to –46 bp; WT or mutant as described below) using the pGL3-promoter vector (Promega).

Oligonucleotides

Oligonucleotides were custom synthesized by MWG Biotech. WT and mutant oligonucleotide probes representing the –58 to –46 bp in the *Fancc* sequence were used for EMSAs: oligo (5′-GCAATTTTCCCG-3′), mutant oligo (5′-GC**CCGG**TTCCCG-3′, with bold representing the mutation). Competitor oligonucleotides from the *Fancf* promoter have been previously described (17).

Murine studies

Irf8$^{+/-}$ mice were obtained from Keiko Ozato (NIH, Bethesda Maryland, USA) (5). *Fancc*$^{+/-}$ mice were a gift from D. Wade Clapp (Indiana University, Indianapolis, Indiana, USA) (34–36).

Bone marrow harvest and culture. Bone marrow mononuclear cells were obtained from the femurs of WT or *Irf8*$^{-/-}$ C57/BL6 mice (5). CD34^{+} cells were separated using the Miltenyi magnetic bead system (Miltenyi Biotechnology). Bipotential GMP cells were cultured (2×10^5 cells/ml) for 48 hours in DME media supplemented with 10% fetal calf serum, 1% pen-strep, 10 ng/ml murine GM-CSF (R&D Systems), 10 ng/ml murine recombinant IL-3 (R&D Systems), and 100 ng/ml SCF (R&D Systems). Cells were either maintained in GM-CSF, IL-3, and SCF for 48 hours or stimulated with G-CSF or IL-1β.

Emergency granulopoiesis. WT, *Fancc*$^{+/-}$, or *Fancc*$^{-/-}$ mice were injected i.p. with Alum or saline control for 4 weeks (10 mice per group). Alum was prepared as described and a 0.5 ml volume was injected i.p. (38). Some cohorts of mice were treated with anakinra (150 mg/kg; Amgen) 24 hours before and 72 hours after Alum (10 mice per group).

Analysis of peripheral blood and bone marrow. Peripheral blood was obtained from the tail vein of each mouse for 2 weeks, and complete blood counts (with leukocyte differential) were determined using an automated cell counter. Myeloid blast counts were verified by hand counting of May-Grunwald-Giemsa–stained peripheral blood smears (blinded for the results of the automated differential; 300 cells counted per slide). Mice were sacrificed if they developed leukocytosis >100,000 cells/ml or a Hgb concentration of ≤6.0. Images of peripheral blood were captured by light microscopy (×40 magnification).

Sternal bone marrow samples were decalcified and stained using hematoxylin and eosin, according to standard techniques, by the Pathology Core Facility of the Robert H. Lurie Comprehensive Cancer Center. Light microscopy was performed, and digital images were captured (×40 magnification).

Serum IL-1β and G-CSF determination. Serum was obtained from the tail veins of WT or *Fancc*$^{-/-}$ mice 2 weeks after i.p. injection with saline or Alum. Serum was analyzed by IL-1β or G-CSF ELISA, and cytokine concentrations were calculated using a commercially available kit (Promega, E-max ImmunoAssay System) according to manufacturer's instructions.

Murine bone marrow transplantation. Bone marrow was harvested from *Fancc*$^{-/-}$ mice 2 weeks after injection of Alum or saline (as described above). LIN$^-$SCA1$^+$ cells were selected from the population of total bone marrow mononuclear cells using magnetic bead–conjugated antibodies (according to manufacturer's instructions; Miltenyi Biotech) (6, 27). Viable cells were obtained by negative selection using Annexin V–conjugated magnetic beads (according to manufacturer's instructions; Miltenyi Biotech). Lethally irradiated WT C57 Black 6 mice were injected (retro-orbital) with LIN$^-$SCA1$^+$ cells (5×10^5 cells plus 10^5 SCA1$^-$ WT bone marrow helper cells).

Apoptosis assays

In situ TUNEL assay. To detect apoptosis of mouse sternum in situ, the labeling reaction was performed using the TACS 2 TdT/DAB in site apoptosis kit according manufacturers' instructions (Trevigen). Briefly, mouse sterna were fixed in formalin for at least 24 hours, decalcified, and then cut into 4-μm sections. Paraffin was removed prior to labeling. After DAB staining, slides were counterstained with eosin staining solution. Tissue sections from 3 mice in each group were used for TUNEL assay, with the total of 12 mice (WT saline control, WT Alum-treated, *Fancc*$^{-/-}$ saline control, and *Fancc*$^{-/-}$ Alum-treated mice). Ten high-powered fields (at ×40) were counted for each sample for positive staining.

Flow cytometry assay. WT or *Fancc*$^{-/-}$ mice were injected i.p. with Alum, and bone marrow was obtained 2 weeks later. Bone marrow cells were washed with PBS, counted, and labeled with anti-mouse FITC-conjugated antibodies to SCA1 (Ly-6A/E), CD34, or GR1 (Ly-6G) (eBioscience). Apoptosis in these cells was assessed by flow cytometry using Annexin V-PE Apoptosis Detection Kit I according to manufacturer's instructions (BD Pharmingen).

Quantitative real-time PCR

RNA was isolated using the TRIzol reagent (Gibco-BRL) and tested for integrity by denaturing gel electrophoresis. Primers were designed with Applied Biosystems software, and real-time PCR was performed using SYBR green according to the "standard curve" method. For all real-time PCR experiments, at least 3 independent samples were evaluated in triplicate.

Results for mRNA expression were normalized to both 18S and actin. No significant difference was found with these 2 genes, and results normalized to 18S are shown. For evaluation of *Fancc*, *Fancf* and *Irf8* mRNA abundance in murine bone marrow cells, cDNA from WT cells that were cultured in GM-CSF, IL-3, and SCF was used to generate the standard curve. For evaluation of these messages in human myeloid cell lines, cDNA from U937 cells that were cultured under standard conditions was used. Results for chromatin immunoprecipitation were normalized to nonprecipitated (control) lysate as input DNA. For these studies, genomic DNA was used to generate the standard curve.

Myeloid cell line transfections and assays

Myeloid cell lines. The human myelomonocytic leukemia cell line U937 (32) was obtained from Andrew Kraft (Hollings Cancer Center, University of South Carolina, Charleston, South Carolina, USA). Cells were maintained as described previously (14–17).

Stable transfectants. U937 cells (32) were transfected by electroporation with equal amounts of an IRF8 expression vector or empty vector (IRF8/pcDNAamp or pcDNAamp) plus a vector with a neomycin phospho transferase cassette (pSRα) (30 μg each). Stable pools of cells were selected in G418 (0.5 mg/ml). At least 3 independent pools of stable transfectants were selected and analyzed.

Fancc reporter assays. U937 cells (32×10^6/ml) were transfected with vectors to express IRF8 or control (50 μg). Cells were cotransfected with a firefly luciferase reporter construct with various sequences from the *Fancc* 5′ flank (20 μg, using the pGL3 vector from Promega) and a CMV/renilla luciferase reporter (10 μg, for transfection efficiency). Empty reporter vector was the control in these experiments.

In other experiments, U937 cells were cotransfected with an artificial promoter construct with 3 copies of the –58- to –46-bp *Fancc* promoter sequence (WT or mutant, as described above) linked to a minimal promoter and firefly luciferase reporter (or control vector without *Fancc* sequence), a vector to express IRF8 (or control vector), and a CMV promoter/renilla luciferase vector. Reporter assays were performed using the dual luciferase reporter system according to manufacturer's instructions (Promega) (14).

DNA repair assays. TK-luciferase reporter vector (Promega) was treated with MMC to generate DNA crosslinks, as previously described (17). U937 cells were stably transfected with a vector to express IRF8-specific shRNAs or with scrambled control vectors. These cells were transiently transfected with reporter vector (with or without MMC pretreatment) and a vector to express FANCC, FANCF, both, or empty vector control. Reporter assays were performed with differentiation with RA/DMF. Results were normalized by cotransfecting with an internal control reporter plasmid (CMV-β-galactosidase).

In vitro DNA-binding assays

Isolation of nuclear proteins. Nuclear proteins were extracted from U937 cells by the method of Dignam with modification, as described previously (17).

EMSAs. Oligonucleotides probes were prepared and EMSAs were performed, as described previously (17). For binding reactions with IRF8 antibody, disruption of the complex (not supershift) was anticipated, based on the location of the epitopes used for antibody production. Binding competition studies were performed with 200-fold molar excess double-stranded synthetic oligonucleotides. For all experiments, at least 3 batches of nuclear proteins were tested in 2 independent experiments. A representative study is shown. Integrity of the nuclear proteins and equality of protein loading are determined in EMSA with a probe representing a classical CCAAT box from the promoter of the α globin gene.

Western blotting

In some experiments, cells were lysed in SDS-sample buffer, as previously described (6, 17). In other experiments, cells were fractionated into the chromatin-enriched versus soluble fractions, as previously described (31). For these studies, cells were lysed in fractionation buffer (10 mM PIPES [pH 6.8], 0.1 M NaCl, 5 mM $MgCl_2$, 1 mM EGTA, 1 mM EDTA, 0.3 M sucrose, 1 mM PMSF, 1 μg/ml leupeptin, 1 μg/ml aprotinin, and 0.1% Triton X-100) for 5 minutes on ice. Lysates were centrifuged at 1,500 *g*, and the supernatant (soluble) fraction was recovered. The pellet (chromatin enriched) was resuspended in fractionation buffer (supplemented to 0.25 M NaCl) and sonicated prior to loading on SDS-PAGE. Western blots were serially probed with antibodies as indicated. Two independent experiments were performed, and a representative blot is shown.

Genomic sequence analysis

Conserved genomic sequences and consensus sequences for interferon

regulatory factor DNA-binding were identified using VISTA software (Genomics Division of the Lawrence Berkeley National Laboratory, Berkeley, California, USA) (50, 51).

Statistics

Statistical significance was determined by unpaired, 2-tailed Student's *t* test (to compare 2 samples), ANOVA (to compare more than 2 samples), or log-rank analysis (to analyze survival curves) using SigmaPlot and SigmaStat software. *P* values of less than 0.04 were considered statistically significant. In all of the graphs, error bars represent ± SEM.

Study approval

Animal studies were performed according to a protocol approved by the Animal Care and Use Committees of Northwestern University and Jesse Brown VA Medical Center.

Acknowledgments

We would like to thank D. Wade Clapp for his gift of *Fancc*$^{+/-}$ mice and for helpful discussions. We would also like to thank Amgen for providing anakinra (Kineret) for these studies. This work was supported by a research grant from the Fanconi Anemia Research Fund, VA Merit Review, and NIH-HL088747 (to E.A. Eklund).

Received for publication January 28, 2013, and accepted in revised form June 13, 2013.

Address correspondence to: Elizabeth A. Eklund, Department of Medicine, The Feinberg School at Northwestern University, 303 E. Superior, Lurie 5-105, Chicago, Illinois 60611, USA. Phone: 312.503.3208; Fax: 312.503.0189; E-mail: e-eklund@northwestern.edu.

1. Driggers PH, et al. An interferon gamma-regulated protein that binds the interferon-inducible enhancer element of major histocompatibility complex class I genes. *Proc Natl Acad Sci U S A*. 1990;87(10):3743–3747.
2. Eklund EA, Jalava A, Kakar R. PU.1, interferon regulatory factor 1, and interferon consensus sequence binding protein cooperate to increase gp91phox expression. *J Biol Chem*. 1998;273(22):13957–13965.
3. Eklund EA, Kakar R. Recruitment of CBP by PU.1, IRF1 and ICSBP is necessary for gp91phox and p67phox expression. *J Immunol*. 1999; 163(11):6095–6105.
4. Kim YM, et al. Roles of IFN consensus sequence binding protein and PU.1 in regulating IL-18 gene expression. *J Immunol*. 1999;163(4):2000–2007.
5. Holtschke T, et al. Immuno-deficiency and chronic myelogenous leukemia-like syndrome in mice with a targeted mutation of the ICSBP gene. *Cell*. 1996;87(2):307–317.
6. Konieczna I, et al. Constitutive activation of SHP2 cooperates with ICSBP-deficiency to accelerate progression to acute myeloid leukemia. *J Clin Invest*. 2008;118(3):853–867.
7. Ueda Y, Cain DW, Kuraoka M, Kondo M, Kelsoe G. IL1R type I dependent hematopoietic stem cell proliferation is necessary for inflammatory granulopoiesis and reactive neutrophilia. *J Immunol*. 2009;182(10):6477–6484.
8. Cain DW, Snowden PB, Sempowski GD, Kelsoe G. Inflammation triggers emergency granulopoiesis through a density-dependent feedback mechanism. *PLoS One*. 2011;6(5):e19957.
9. Hirai H, et al. C/EBPbeta is required for 'emergency' granulopoiesis. *Nat Immunol*. 2006;7(7):732–739.
10. Panopoulos AD, et al. Stat3 governs distinct pathways in emergency granulopoiesis and mature neutrophils. *Blood*. 2006;108(12):3682–3690.
11. Lieschke GJ, et al. Mice lacking G-CSF have chronic neutropenia, granulocyte and macrophage progenitor cell deficiency and impaired neutrophil mobilization. *Blood*. 1994;84(6):1737–1746.
12. Zhan Y, Lieschke GJ, Grail D, Dunn AR, Cheers C. Essential roles for GM-CSF and G-CSF in the sustained hematopoietic response of Listeria monocytogenes infected mice. *Blood*. 1998;91(3):863–869.
13. Panopoulos AD, Watchwich SS. Granulocyte colony stimulating factor: molecular mechanisms of activation during steady state and emergency hematopoiesis. *Cytokine*. 2008;42(3):277–288.
14. Huang W, Saberwal G, Horvath E, Zhu C, Lindsey S, Eklund EA. Leukemia associated, constitutively active mutants of SHP2 protein tyrosine phosphatase inhibit NF1-transcriptional activation by the interferon consensus sequence binding protein. *Mol Cell Biol*. 2006;26(17):6311–6332.
15. Huang W, Zhu C, Wang H, Horvath E, Eklund EA. The interferon consensus sequence binding protein (ICSBP/IRF8) represses PTPN13 gene transcription in differentiating myeloid cells. *J Biol Chem*. 2008;283(12):7921–7935.
16. Huang W, et al. The Interferon consensus sequence binding protein (ICSBP) decreases beta-catenin activity in myeloid cells by repressing GAS2 transcription. *Mol Cell Biol*. 2010;30(19):4575–4594.
17. Saberwal G, Horvath E, Hu L, Zhu C, Hjort E, Eklund EA. The interferon consensus sequence binding protein (ICSBP/IRF8) activates transcription of the *FANCF* gene during myeloid differentiation. *J Biol Chem*. 2009;284(48):33242–33254.
18. Moldovan GL, D'Andrea AD. How the fanconi anemia pathway guards the genome. *Annu Rev Genet*. 2009;43:223–249.
19. Kee Y, D'Andrea AD. Molecular pathogenesis and clinical management of Fanconi anemia. *J Clin Invest*. 2012;122(11):3799–3806.
20. Thompson LH, Hinz JM. Cellular and molecular consequences of defective Fanconi anemia proteins in replication-coupled DNA repair: mechanistic insights. *Mut Res*. 2009;668(1–2):54–72.
21. Li X, Heyer WD. Homologous recombination in DNA repair and DNA damage tolerance. *Cell Res*. 2008;18(1):99–113.
22. Schlacher K, Wu H, Jasin M. A distinct replication fork protection pathway connects Fanconi Anemia tumor suppressors to Rad51-BrCA1/2. *Cancer Cell*. 2012;22(1):106–116.
23. Wang LC, Stone S, Hoatlin ME, Gautier J. Fanconi anemia proteins stabilize replication forks. *DNA Repair (Amst)*. 2008;7(12):1973–1981.
24. Taniguchi T, Garcia-Higuera I, Andreassen PR, Gregory RC, Grompe M, D'Andrea AD. S-phase specific interaction of the Fanconi anemia protein, FANCD2, with BRCA1 and RAD51. *Blood*. 2002;100(7):2414–2420.
25. Auerbach AD, Allen RG. Leukemia and preleukemia in Fanconi anemia patients. A review of the literature and report of the International Fanconi Anemia Registry. *Cancer Genet Cytogenet*. 1991;51(1):1–12.
26. Cioc AM, Wagner JE, MacMillan ML, DeFor T, Hirsch B. Diagnosis of myelodysplastic syndrome among a cohort of 119 patients with Fanconi Anemia. *Am J Clin Pathol*. 2010;133(1):92–100.
27. Wang H, et al. Constitutively active SHP2 cooperates with HoxA10 overexpression to induce acute myeloid leukemia. *J Biol Chem*. 2009;284(4):2549–2567.
28. Zhu CL, Saberwal G, Lu YF, Platanias LC, Eklund EA. The interferon consensus sequence binding protein (ICSBP) activates transcription of the gene encoding Neurofibromin 1 (NF1). *J Biol Chem*. 2004;279(49):50874–50885.
29. Scheller M, et al. Altered development and cytokine responses of myeloid progenitors in the absence of transcription factor, interferon consensus sequence binding protein. *Blood*. 1999;94(11):3764–3771.
30. Holtschke T, et al. Immuno-deficiency and chronic myelogenous leukemia-like syndrome in mice with a targeted mutation of the ICSBP gene. *Cell*. 1996;87(2):307–317.
31. Kin JM, Kee Y, Gurtan A, D'Andrea AD. Cell cycle-dependent chromatin loading of the Fanconi anemia core complex by FANCM/FAAP24. *Blood*. 2008;111(10):5215–5222.
32. Larrick JW, Fischer DG, Anderson SJ, Koren HA. Characterization of a human macrophage-like cell line stimulated to differentiate in vitro: a model of macrophage functions. *J Immunol*. 1980;125(1):6–12.
33. Levy DE, Kessler DS, Pine R, Reich N, Darnell JE Jr. Interferon-induced nuclear factors that bind a shared promoter element correlate with positive and negative transcriptional control. *Genes Dev*. 1988;2(4):383–393.
34. Chen M, et al. Inactivation of FANC in mice produces inducible chromosomal instability and reduced fertility reminiscent of Fanconi Anaemia. *Nat Genet*. 1996;12(4):448–451.
35. Carreau M, Gan OI, Liu L, Doedens M, Dick JE, Buchwald M. Hematopoietic compartment of Fanconi anemia group C null mice contains fewer lineage-negative CD34+ primitive hematopoietic cells and shows reduced reconstruction ability. *Exp Hematol*. 1999;27(11):1667–1674.
36. Carreau M, et al. Bone marrow failure in the Fanconi anemia group C mouse model after DNA damage. *Blood*. 1998;91(8):2737–2744.
37. Freie B, et al. Fanconi anemia type C and p53 cooperate in apoptosis and tumorigenesis. *Blood*. 2003;102(12):4146–4152.
38. Kool M, et al. Cutting edge: alum adjuvant stimulates inflammatory dendritic cells through activation of the NALP3 inflammasome. *J Immunol*. 2008;181(6):3755–3759.
39. Basu S, Hodgson G, Zhang HH, Katz M, Quilici C, Dunn AR "Emergency" granulopoiesis in G-CSF-deficient mice in response to Candida albicans infection. *Blood*. 2000;95(12):3725–3733.
40. Zhan Y, Lieschke GJ, Grail D, Dunn AR, Cheers C. Essential roles for GM-CSF and G-CSF in the sustained hematopoietic response of Listeria monocytogenes infected mice. *Blood*. 1998;91(3):863–869.
41. Ueda Y, Yang K, Foster SJ, Kondo M, Kelsoe G. Inflammation controls B lymphopoiesis by regulating chemokine CXCL12 expression. *J Exp Med*. 2004;199(1):47–58.
42. Arend WP. Interleukin 1 receptor antagonist. A new member of the interleukin 1 family. *J Clin Invest*. 1991;88(5):1445–1451.
43. Fleishmann RM. Safety of anakinra, a recombinant interleukin-1 receptor antagonist (r-metHuIL-1ra), in patients with rheumatoid arthritis and comparison to anti-TNF-alpha agents. *Clin Exp Rheumatol*. 2002;20(5 suppl 27):S35–S41.
44. de Oliveira-Junior EB, Bustamante J, Newburger

PE, Condino-Neto A. The human NADPH oxidase; primary and secondary defects impairing the respiratory burst function and the microbicidal ability of phagocytes. *Scand J Immunol*. 2011;73(5):420–427.
45. Rathbun RK, et al. Inactivation of the Fanconi anemia group C gene augments interferon-gamma-induced apoptotic responses in hematopoietic cells. *Blood*. 1997;90(3):974–985.
46. Haneline LS, et al. Multiple inhibotry cytokines induce deregulated progenitor growtn and apoptosis in hematopietic cells from Fanc$^{-/-}$ mice. *Blood*. 1998;91(11):4092–4098.
47. Kang KW, Kim TS, Kim KM. Interferon gamma and interleukin 4 targeted gene therapy for atopic allergic disease. *Immunology*. 1999;97(3):462–465.
48. Ibáñez A, Río P, Casado JA, Bueren JA, Fernández-Luna JL, Pipaón C. Elevated levels of IL-1beta in Fanconi anaemia group A patients due to a constitutively active phosphoinositide 3-kinase-Akt pathway are capable of promoting tumour cell proliferation. *Biochem J*. 2009;422(1):161–170.
49. Surguladze D, et al. Tumor necrosis factor-alpha and interleukin-1 antagonists alleviate inflammatory skin changes associated with epidermal growth factor receptor antibody therapy in mice. *Cancer Res*. 2009;69(14):5643–5647.
50. Mayor C, et al. VISTA: visualizing global DNA sequence alignments of arbitrary length. *Bioinformatics*. 2000;16(11):1046–1047.
51. Loots G, Ovcharenko I, Pachter L, Dubchak I, Rubin EM. rVista for comparative sequence-based discovery of functional transcription factor binding sites. *Genome Res*. 2002;12(5):832–839.